

NASA/CR-2014-218526



# Colombia Mi Pronóstico Flood Application: Updating and Improving the Mi Pronóstico Flood Web Application to Include an Assessment of Flood Risk

*Stephanie Rushley, Matthew Carter, Charles Chiou, Richard Farmer, Kevin Haywood, Anthony Pototzky Jr., Adam White, and Daniel Winker  
Langley Research Center, DEVELOP National Program, Hampton, Virginia*

---

September 2014

## NASA STI Program . . . in Profile

Since its founding, NASA has been dedicated to the advancement of aeronautics and space science. The NASA scientific and technical information (STI) program plays a key part in helping NASA maintain this important role.

The NASA STI program operates under the auspices of the Agency Chief Information Officer. It collects, organizes, provides for archiving, and disseminates NASA's STI. The NASA STI program provides access to the NASA Aeronautics and Space Database and its public interface, the NASA Technical Report Server, thus providing one of the largest collections of aeronautical and space science STI in the world. Results are published in both non-NASA channels and by NASA in the NASA STI Report Series, which includes the following report types:

- **TECHNICAL PUBLICATION.** Reports of completed research or a major significant phase of research that present the results of NASA Programs and include extensive data or theoretical analysis. Includes compilations of significant scientific and technical data and information deemed to be of continuing reference value. NASA counterpart of peer-reviewed formal professional papers, but having less stringent limitations on manuscript length and extent of graphic presentations.
- **TECHNICAL MEMORANDUM.** Scientific and technical findings that are preliminary or of specialized interest, e.g., quick release reports, working papers, and bibliographies that contain minimal annotation. Does not contain extensive analysis.
- **CONTRACTOR REPORT.** Scientific and technical findings by NASA-sponsored contractors and grantees.

- **CONFERENCE PUBLICATION.** Collected papers from scientific and technical conferences, symposia, seminars, or other meetings sponsored or co-sponsored by NASA.
- **SPECIAL PUBLICATION.** Scientific, technical, or historical information from NASA programs, projects, and missions, often concerned with subjects having substantial public interest.
- **TECHNICAL TRANSLATION.** English-language translations of foreign scientific and technical material pertinent to NASA's mission.

Specialized services also include organizing and publishing research results, distributing specialized research announcements and feeds, providing information desk and personal search support, and enabling data exchange services.

For more information about the NASA STI program, see the following:

- Access the NASA STI program home page at <http://www.sti.nasa.gov>
- E-mail your question to [help@sti.nasa.gov](mailto:help@sti.nasa.gov)
- Fax your question to the NASA STI Information Desk at 443-757-5803
- Phone the NASA STI Information Desk at 443-757-5802
- Write to:  
STI Information Desk  
NASA Center for AeroSpace Information  
7115 Standard Drive  
Hanover, MD 21076-1320

NASA/CR–2014-218526



# Colombia Mi Pronóstico Flood Application: Updating and Improving the Mi Pronóstico Flood Web Application to Include an Assessment of Flood Risk

*Stephanie Rushley, Matthew Carter, Charles Chiou, Richard Farmer, Kevin Haywood, Anthony Pototzky Jr., Adam White, and Daniel Winker  
Langley Research Center, DEVELOP National Program, Hampton, Virginia*

National Aeronautics and  
Space Administration

Langley Research Center  
Hampton, Virginia 23681-2199

Prepared for Langley Research Center  
under Contract NNX14AB604

September 2014

Available from:

NASA Center for Aerospace Information  
7115 Standard Drive  
Hanover, MD 21076-1320  
443-757-5802

## I. Abstract

Colombia is a country with highly variable terrain, from the Andes Mountains to plains and coastal areas, many of these areas are prone to flooding disasters. To identify these risk areas NASA's Advanced Spaceborne Thermal Emission and Reflection Radiometer (ASTER) was used to construct a digital elevation model (DEM) for the study region. The preliminary risk assessment was applied to a pilot study area, the La Mosca River basin. Precipitation data from the National Aeronautics and Space Administration (NASA) Tropical Rainfall Measuring Mission (TRMM)'s near-real-time rainfall products as well as precipitation data from the Instituto de Hidrologia, Meteorología y Estudios Ambientales (the Institute of Hydrology, Meteorology and Environmental Studies, IDEAM) and stations in the La Mosca River Basin were used to create rainfall distribution maps for the region. Using the precipitation data and the ASTER DEM, the web application, Mi Pronóstico, run by IDEAM, was updated to include an interactive map which currently allows users to search for a location and view the vulnerability and current weather and flooding conditions. The geospatial information was linked to an early warning system in Mi Pronóstico that can alert the public of flood warnings and identify locations of nearby shelters.

## II. Introduction

Colombia is prone to frequent flooding due to heavy precipitation that is influenced by the Intertropical Convergence Zone (ITCZ) and the Andes Mountain range [Colombia-SA, 2014] which causes precipitation patterns to be dominated by orographic lift [Poveda, Álvarez, and Rueda, 2011; Poveda et al., 2005]. Due to the high amount of precipitation that falls over Colombia and the highly variable slopes, Colombia's mountainous regions are highly prone to floods and landslides, which has caused hundreds of deaths in the area over the past ten years [Künzler, Huggel, and Ramírez, 2012]. Currently, Colombia's Instituto de Hidrologia, Meteorología y Estudios Ambientales (Institute of Hydrology, Meteorology and Environmental Studies, IDEAM) has the Mi Pronóstico web and mobile application which notifies people where there is a flood warning.

The DEVELOP Tech Team is addressing the DEVELOP national application area cross-cutting to create a flood risk assessment map for the La Mosca river basin. The La Mosca River watershed, which is located in the southern portion of the Antioquia Department in Northwest Colombia served as a pilot study area for an updated flood risk assessment and warning system. The flood risk map will provide information for planning future regional development and land use [Spachinger et al., 2008] as well as provide current watches and warnings. The DEVELOP Tech Team has partnered with IDEAM, which has provided rain gauge and streamflow data for the purpose of expanding the Mi Pronóstico web application. Using TRMM and DRIVE will allow for near-real-time monitoring of precipitation for the purpose of flood warning and preparation.

Topography is an important factor in causing precipitation as well as determining the flow of water once it reaches the ground. Several digital elevation models (DEMs) exist, including two NASA open source global DEMs (GDEMs), from the Shuttle Radar Topography Mission (SRTM) and from the Advanced Spaceborne Thermal Emission and Reflection Radiometer (ASTER) aboard the Terra satellite. The SRTM GDEM is publicly available at a 3 arc-second resolution for Colombia [Nikolakopoulos, Kamaratakis, and Chrysoulakis, 2006]. SRTM has voids and gaps within the GDEM [Tighe and Chamberlain, 2009]. Various interpolation methods exist for filling these voids, however, the accuracy of the interpolated elevations has been shown to be poor quality [Zhao and Ling, 2010].

ASTER has been collecting along-track stereo images since 2000 using a pair of infrared cameras [Tachikawa et al, 2011]. The ASTER GDEM has a 1 arc second horizontal resolution and was created by processing the 1.26 million scenes of Level-1A data [Czubski, Kozak, and Kolecka, 2013; Tachikawa et al, 2011]. The ASTER GDEM also has voids, mostly due to cloud cover, but they are limited because of the size of the dataset. In processing cloud pixels are removed from the scenes, then scenes of the same area are stacked [Zhao and Ling, 2010]. A higher number of scenes used to produce a DEM correlates with a smaller error, especially for DEMs produced from between one and ten scenes [Tachikawa et al, 2011]. The ASTER GDEM has a generally higher spatial resolution and fewer voids [Zhao and Ling, 2010], therefore, the ASTER DEM was used for the study.

South America has some of the most intense Deep moist convection (DMC) in the world and accumulates a high amount of precipitation [Rasmussen et al., 2013]. DMC is caused by moisture from the Pacific Ocean to the west and the Amazon River Basin to the east that is lifted by the winds interacting with the mountains [Poveda, Álvarez, and Rueda, 2011]. As a result the variable topography plays a large role in the daily variation of local precipitation [Poveda et al., 2005]. The location and timing of precipitation is critical to any kind of hydrological model, especially for flood risk analysis.

In addition to orographic lift due to local topography, precipitation is highly affected by large scale tropical dynamics. Colombia gets a double passage of the (ITCZ), first in March, April and May and again in September, October and November, causing a significant amount of precipitation during these two seasons [Poveda, Álvarez, and Rueda, 2011]. Phase changes in the El-Niño – Southern Oscillation (ENSO) cause wide spread teleconnections, which influence precipitation patterns in Colombia. Trends have shown that during the El Niño (warm) phase, precipitation accumulation over most of Colombia is relatively low, while during the La Niña (cold) phase, precipitation amounts are typically high [Poveda, Álvarez, and Rueda, 2011; Poveda et al., 2005]. Although precipitation in Colombia shows a high amount of spatial and seasonal variability, strong diurnal patterns are present. Local minimums in precipitation accumulation occur in the morning, regardless of season and location, while local maximums vary by location. Northeastern and Western Colombia experience a peak in precipitation during the afternoon, while west of the Andes Mountains peaks occurs around local midnight [Poveda et al., 2005].

Any change in precipitation due to climate and land use around a river can cause changes to flooding patterns [Spachinger et al., 2008]. An increased necessity for a more accurate and detailed flood risk analysis in Colombia has arisen because of increased frequency of significant flooding events whose magnitude and impact have been further exacerbated by development along Colombia's rivers [Mosquera-Machado and Ahman, 2007]. Floods result from a chain of events that starts with meteorological and hydrological factors that can be amplified by human factors [Mrekva and Engi, 2012; Spachinger et al., 2008]. Meteorological factors include accumulated rainfall, storm type and size, and temperature. The chronological events preceding the precipitation event are large because the amount of runoff from these storms is dictated by the current water level, moisture content of soil, infiltration of surfaces, and where the runoff is coming from. The ability of water to infiltrate surfaces, which helps to mitigate flooding, is lessening due to the development of cities in flood plains which causes large areas of land to be covered with impermeable surfaces [Mrekva and Engi, 2012; Spachinger et al., 2008].

Due to the importance of precipitation to hydrological modeling, the National Aeronautics and Space Administration's (NASA) Tropical Rainfall Measuring Mission (TRMM) Multi-Satellite Precipitation Analysis (TMPA) near-real-time dataset, 3B42RT, was used to get consistent precipitation information [Wu et al., 2014]. TRMM was launched in 1997 and provides measurements for the tropics (50S to 50N). TRMM carries a spaceborne precipitation radar which examines the vertical structure of precipitation in a swath 215km long and 4.3km wide [Kawanishi et al., 2000]. Precipitation must be at a minimum of 0.7mm/hr for the spaceborne precipitation radar to detect it. The precipitation radar is calibrated to a less than 1 dBZ error [Kawanishi et al., 2000]. TRMM passes over the same area two to four times a day; however, due to the cycle for small locations, such as La Mosca River, data is received less frequently, which requires that it be corrected with in-situ data. In a study of the Himalayas Bookhagen and Burbank (2006) found this correction to be a constant scaling factor.

The TRMM near-real time data set does not use gauge adjustment for the purpose of having a shorter lag time [Dinku et al., 2009]. This dataset is known to have a high level of error [Dinku et al., 2009]; however, with a limited amount of in situ measurements in Colombia [Mosquera-Machado and Ahmad, 2007], satellite observations from TRMM are the best available source for modeling severe flood events in tropical countries. In addition, it has been shown to be relatively accurate in the Dominant river- tracing routing integrated with VIC (Variable Infiltration Capacity) Environment model (DRIVE) [Wu et al., 2014]. Therefore, TRMM will be used as a substitute for the real time precipitation data for the flood application, in addition to the Global Flood Monitor System (GFMS) created by Wu et al (2014) to look at severe flooding events using TMPA.

Previous studies have pointed out several errors specific to TRMM precipitation in Colombia. In addition to the high level of error found by Dinku et al. (2009), TRMM has a low correlation coefficient of 0.48mm/day and has a magnitude of underestimation of 0.7mm/day [Dinku et al., 2009]. Rasmussen et al. (2013) found that the precipitation radar on TRMM is the cause for significant underestimation of rainfall during DMC events. TRMM's 2A25 algorithm gives inconsistent estimates of precipitation, in particular with DMC where the horizontal 40dBZ core extends above the 0°C level. This

is due to presence of mixed hydrometeors in tandem with the assumption by TRMM's algorithm to correct freezing precipitation to snow particles, which does not accurately depict the hail or graupel present in severe convection [*Rasmussen et al., 2013*]. Taking this information into account we have used the in-situ precipitation gauge data from IDEAM to set the risk indices and check the accuracy of TRMM in La Mosca river basin.

### III. Methodology

#### Data Acquisition

Topographical data for the study area was acquired from the ASTER GDEM2. The data was distributed in GeoTIFF and was ordered through NASA Reverb, Global Data Explorer. The DEM files were produced by Japan's Sensor Information Laboratory Corporation (SILC) from the ASTER Level-1A archive [Land Processes, 2014].

Streamflow rate measurements from 43 river monitoring stations and precipitation measurements from 102 weather stations within Colombia's national network of observation stations were provided by IDEAM from January 1st, 1900 to December 31st, 2013. A number of the stations data only included monthly measurements, only the station's with both daily and monthly data were used in the study. Data was therefore used from 43 stations.

Additionally, near real-time precipitation data from TRMM was used to complement Colombia's national network of observation stations. The TRMM 3B42RT data was obtained from NASA Giovanni data access portal operated out of Goddard Space Flight Center. TRMM outputs precipitation data with a 0.25° grid spacing over the tropics. In addition to Giovanni, the TRMM open source public directory was used to access the gridded binary data files and input those images into ArcGIS. Flood intensity data was gathered from the GFMS DRIVE model, which outputs flooding intensity in millimeters over a flooding threshold [Wu *et al.*, 2014].

#### Data Processing

In order to obtain a continuous DEM for the study area, four ASTER images were mosaicked together. The ArcGIS Hydro Toolbox was used to create a watershed from the ASTER DEM and calculate its area, flow direction, and accumulation. With this a stream mask for the watershed was created. Using the Stream Order tool in ArcGIS, major intersections of flow in the watershed were identified and pour points were set to separate the watershed into seven sub basins.

For calculating the correlation between streamflow and precipitation, flow stations were used as the limiting factor. The daily and monthly streamflow stations were connected to the closest daily and monthly precipitation stations, respectively, by using a function in ArcGIS to find the closest station. The data from these pairs was combined to match flow and precipitation measurements for each day and for each month, missing values were eliminated, and the correlation for each pair was calculated. Additionally correlograms were created for the precipitation and streamflow stations [Friendly, 2002]. After data processing, several stations were eliminated due to missing values, leaving us with 19 station data points for the correlation calculations.

#### Data Analysis

Once the closest precipitation station to each streamflow station was determined, the precipitation-streamflow station pairs were used to calculate the correlation coefficient between both precipitation and streamflow and between the streamflow and slope in order to assess any linear correlation (Appendix 1). Additionally, autocorrelations were calculated for the streamflow and precipitation data to look for recurring time

dependent trends. Cross-correlations were used to examine the precipitation-streamflow relationship. A cross-correlation as opposed to a simple correlation coefficient calculation can account for a lag in the relationship, for example if streamflow is more affected by rainfall from days earlier [Friendly, 2002]. Künzler, Huggel, and Ramírez (2012) found that when data covering long periods of time (100 years or greater) were used, the discharge patterns were highly dependent on the statistical methods used. Therefore, only twenty years of data, from 1993 to 2013, were used in this analysis.

Morphometric Index	Scale	Area of Drainage Basin (km <sup>2</sup> )	Categories				
			1	2	3	4	5
Drainage Density (km/km <sup>2</sup> )	1:10,000	<15	<1.50	1.51-2.00	2.01-2.50	2.51-3.00	>3
	1:25,000	16 - 50	<1.20	1.21-1.80	1.81-2.00	2.01-2.50	>2.5
	1:100,000	>50	<1.00	1.01-1.50	1.51-2.00	2.01-2.50	>2.5
			Low	Moderate	Moderate High	High	Very High
Mean Basin Slope (%)	1:10,000	<15	<20	21-35	36-50	51-75	>75
	1:100,000	>50	<15	16-30	30-45	46-65	>65
			Hilly	Strong	Very strong	Steep	Very Steep
Coefficient of Shape			>1.625	1.376-1.500	1.251-1.375	1.126-1.250	1.00-1.125
			Oval-oblong to oblong rectangular	Oval-round to oval-oblong		Almost round to oval-round	

The Morphometric Classification Torrential Index (MCTI) set by IDEAM incorporates the drainage density, slope of the basin, and the shape of the basin [IDEAM, 2013]. By separating the watershed into sub basins, it was possible to examine the different areas for varying levels of flood risk. Each sub basin was calculated to find the individual categories and the risk associated with MCTI. Table 1 shows the different risk value criteria for MCTI. The corresponding risk color associated with the combination of all three indices is shown in Figure 1. The Index of Variability was calculated from the flow duration curves which show the percentage of time that the flow is above a certain value. Table 2 shows the vulnerability that is determined based on the index of variability (untranslated figures can be found in Appendix 2).

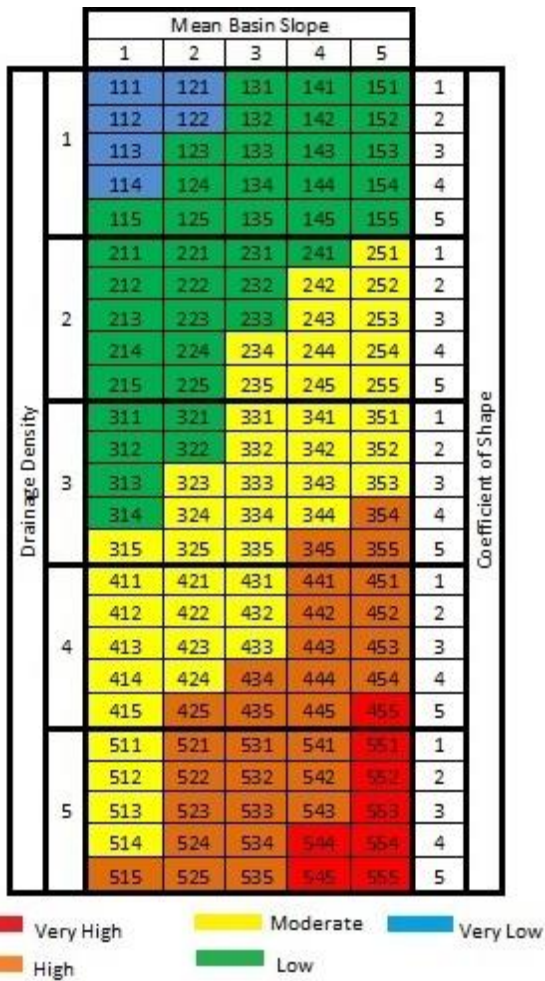


Figure 1: Once all of the indices have been put together they are combined to determine the risk assessment. This determines the MCTI [IDEAM, 2013]

Variability Index	Vulnerability
<10°	Very low
10.1° - 37°	Low
37.1° - 47°	Medium
47.1° - 55°	High
>55°	Very high

Table 2: Vulnerability values based on the variability index.

Once the Index of Variability and the MCTI has been determined, the final Vulnerability Index of Torrential Events (VITE) can be determined. The VITE shows flood risk based on the hydrological features of the basin and the historical flow percentage. These criteria show the risk of the watershed and sub basins to flooding in the event of a significant rain event. Table 3 shows the final criteria for the final Index that will give the VITE.

Table 3: Vulnerability Index of Torrential Events.

Variability Index	Morphometric Classification Torrential Index				
	Very Low	Low	Medium	High	Very High
Very low	Low	Low	Medium	High	High
Low	Low	Medium	Medium	High	Very High
Medium	Low	Medium	High	High	Very High
High	Medium	Medium	High	Very High	Very High
Very high	Medium	High	High	Very High	Very High

## IV. Results & Discussion

### Analysis of Results

The streamflow stations were used as the limiting factor for calculating the correlation between streamflow and precipitation, precipitation and slope, and stream flow and slope (Appendix 1). Correlation between streamflow and precipitation is relatively low for many of the daily stations, with few higher than 0.5, one of which is a daily station (23087130) located nearly 2 km from the closest precipitation station. Correlations for the monthly data were much higher with more stations above 0.5 than below. These correlations are good for hydrological purposes and it appears that when the time scale is increased from daily to monthly, trends arise and the distance between stations seems to have less of an influence. Correlation between slope and precipitation and slope and streamflow had a correlation of magnitude of  $10^{-15}$ , which is to be expected because the precipitation and streamflow data changes over time where, for the purposes of this study, the time scale was small enough that it can be assumed that slope is constant over the study period. Potentially the correlation between streamflow and precipitation could have been negatively affected by the topography, the interaction of rain that falls over areas not covered by precipitation gauges or missing data from several gauges.

## La Mosca Watershed and Subbasins

Data Source: ASTER, DIVA-GIS, and IDEAM

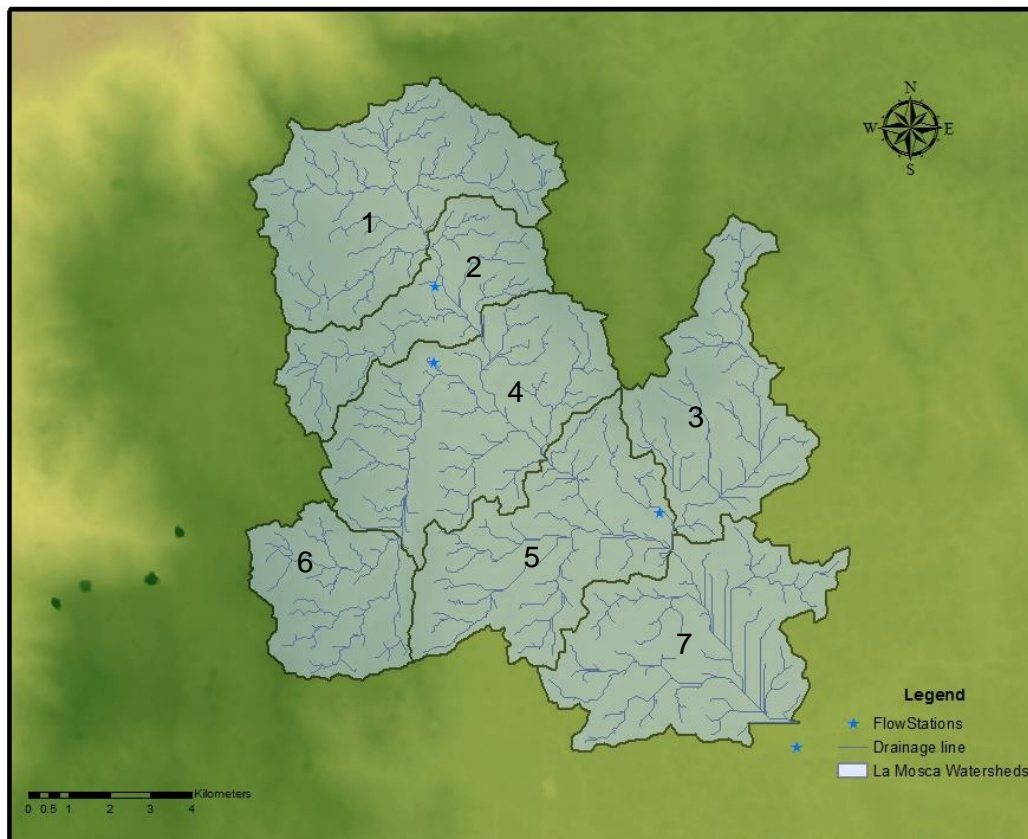


Figure 2: La Mosca Watershed and sub basins that were calculated from ArcGIS. Flow stations, shown as blue stars on this map, were used to compute the flow duration curve and Index of Variability. Station 23087860 is in sub basin 2, Station 23087170 is in sub basin 4, Station 23087030 is the station in sub basin 5, and Station 23087670 is to the south of the watershed.

The correlograms illustrate how the stations are correlated (Appendix 3). The time series correlation plots have shown that there is very little correlation but there is a clear positive and negative pattern that arises in the different seasons. This may be indicative of smaller rainfall amounts in different seasons and therefore a smaller volume of streamflow in those seasons (Figure 3). Not only do these show oscillation in different seasons, but minimums in streamflow correspond well with minimums in precipitation. The time lag shows that the highest correlation is between the precipitation on a day and streamflow a day later; this indicates that there is a lag in the time that it takes for the streamflow to increase with rainfall (Figure 4). Therefore, the potential for flooding does not end when the precipitation ends.

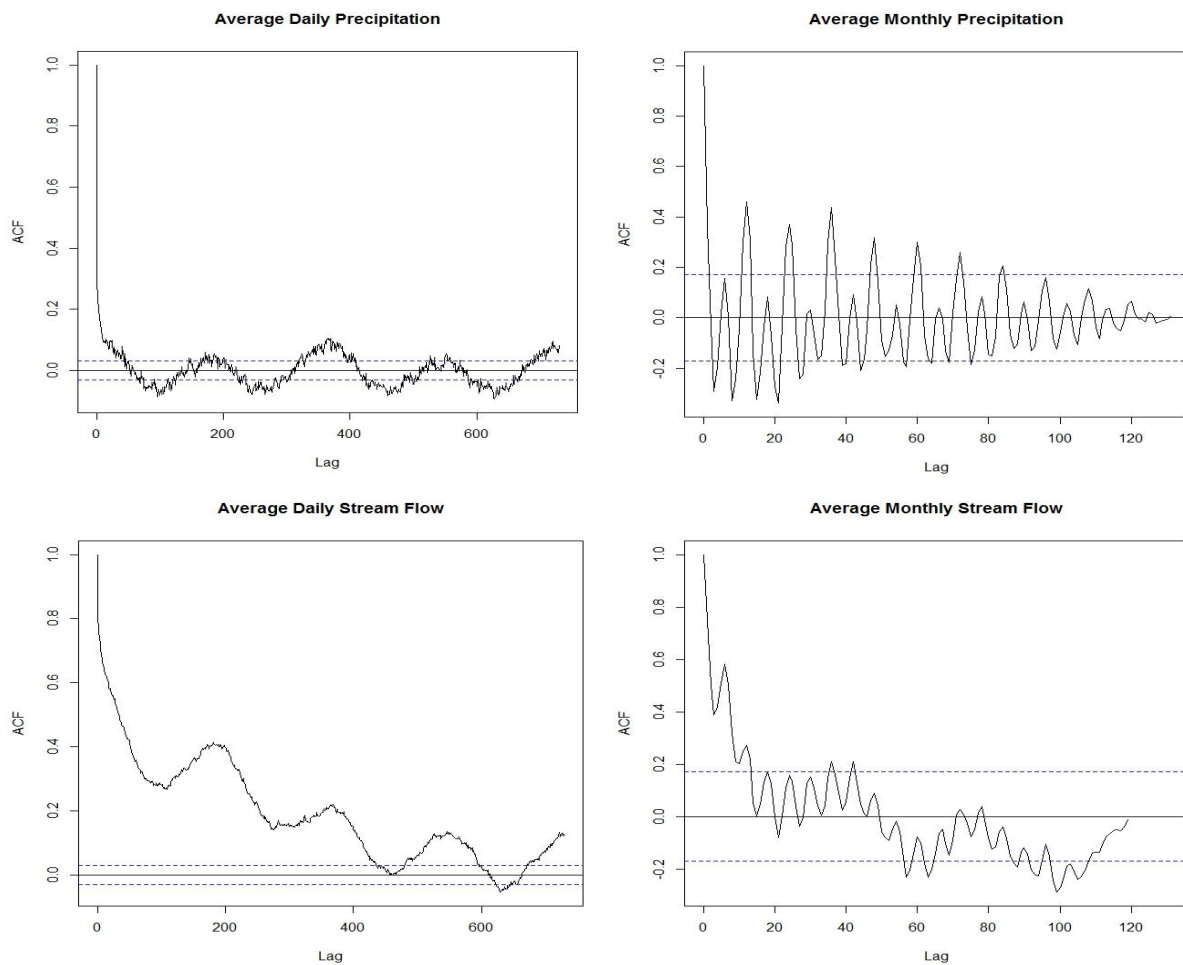


Figure 3: The seasonal time series correlations for daily precipitation and streamflow and monthly precipitation and streamflow.

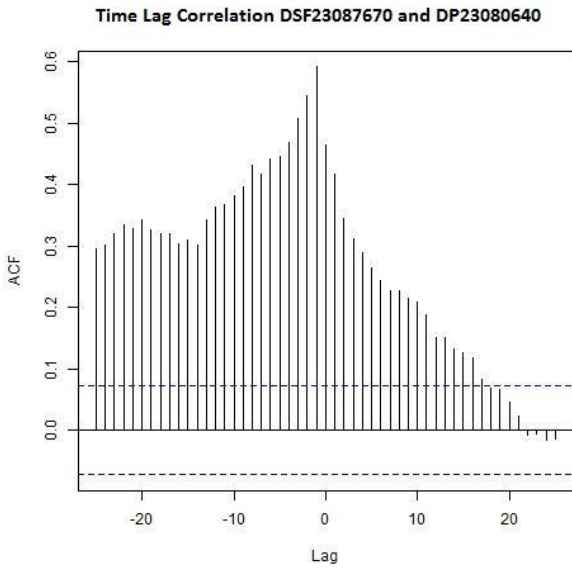


Figure 4: Time lag correlation between Daily Streamflow Station 23087670 and Daily Precipitation Station 23080640.

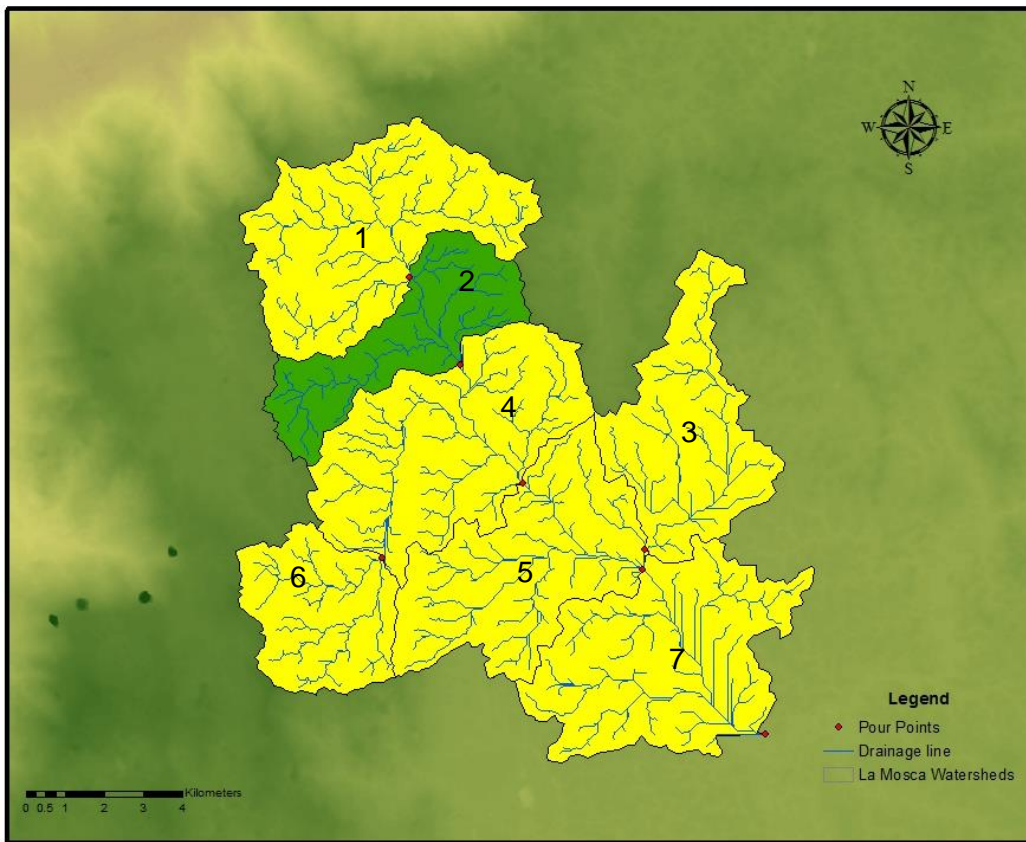


Figure 5: MCTI, colors correspond to the colors in Figure 1.

Figure 5 shows the watershed values based on the MCTI described in Figure 1. This indicates an overall moderate risk throughout the watershed, with a lower risk in sub basin 2. The La Mosca River Basin is more susceptible to flooding in areas where the risk is moderate and should be watched closely when heavy rainfall occurs.

The flow duration curves show the percentage of time that the flow is over a certain value at each of the four stations that are within the watershed (Figure 6). The stations correspond with the stars on the map in Figure 2. The flow stations were connected with the watersheds that flowed most directly into them. The limited number of stations and the distance between the flow stations and pour points create added uncertainty. However, the index of variability is similar to the process completed by IDEAM [IDEAM, 2013]. The Index of Variability (Table 4) is low for most of the stations, with Station 23087860 and Station 23087030, being in the medium range for the smaller percentage ranges. Overall, this creates a low Index of Variability for the entire watershed; additionally the average Index of Variability for all stations is in the low range. Once the MCTI has been determined and the Index of Variability calculated, these two values are put together to get the VITE (Table 3). Combined the moderate MCTI and the low Index of Variability, most sub basins have a medium VITE. Sub basin 2 has a low MCTI and a low Index of Variability, which also gives a medium VITE.

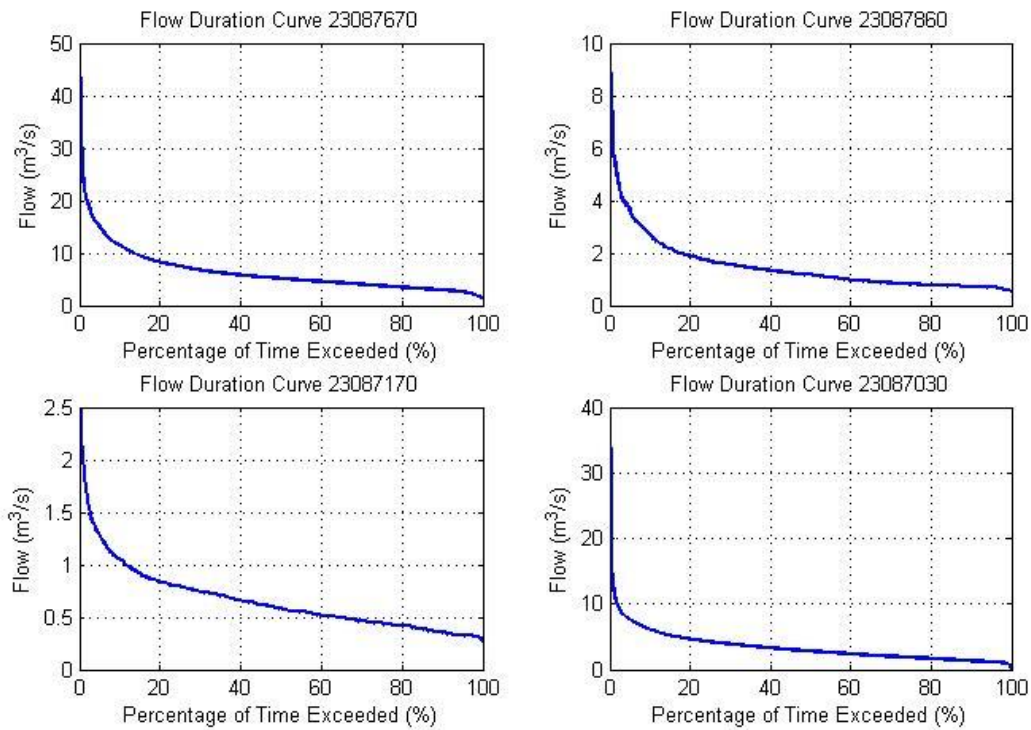


Figure 6: Flow duration curves for the stations within the watershed.

Variability Index	Station 23087670	Station 23087860	Station 23087170	Station 23087030
40%-60%	30.2022	38.9326	30.4553	38.2458
30%-70%	31.7183	35.2720	29.2970	38.0296
20%-80%	32.0733	32.8636	27.3563	36.2351
10%-90%	31.5347	31.0470	26.5651	34.7007

Table 4: The Index of variability, green colors indicate a low vulnerability and yellow colors indicate a medium vulnerability.

Once the watershed areas and their vulnerability were calculated precipitation data from TRMM and flood intensity data from the DRIVE model was overlaid to provide information on current weather to assist in assessing risk within the study area. The data is coarse and therefore just an option for the user of the Mi Pronóstico application to toggle on and off. Shown in Figure 7 are the DRIVE model and TRMM precipitation data over Colombia on July 5<sup>th</sup>, 2014 at 0900Z. The La Mosca Watershed (outlined by the red boxes in Figure 7) is relatively small which makes the pixel size for these products a bad representation for the area. It can be seen that the DRIVE model gives a greater value for the flooding intensity in area with higher precipitation, due to the coarse yet visual appeal of TRMM and DRIVE they will be an option for users of the Mi Pronóstico web application to view, but not used for analysis. This information can be redownloaded and updated on the Mi Pronóstico web application.

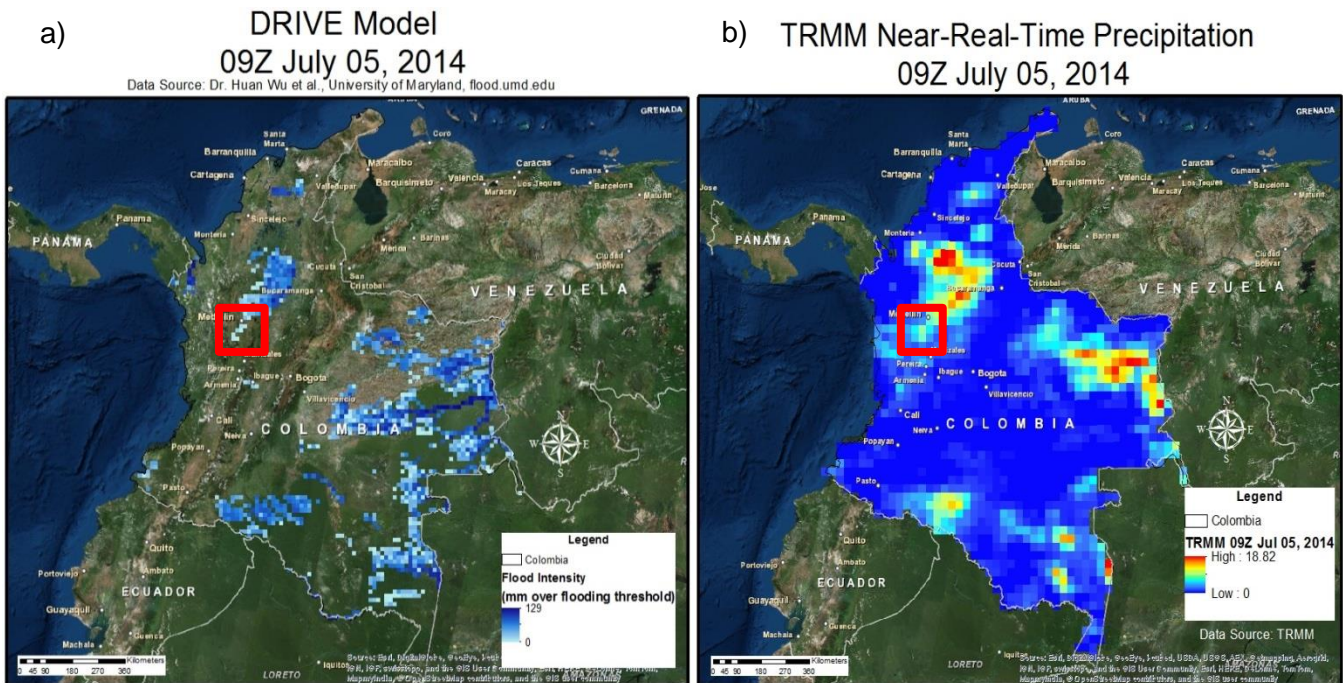


Figure 7: On July 05, 2014 at 0900Z. a) The flooding intensity (mm over threshold) as determined by the DRIVE model from the University of Maryland and b) the TRMM near-real-time precipitation data in mm/hr.

### Errors & Uncertainty

Large errors exist because of the large amount of missing data in the streamflow and precipitation data as well as the sparse amount of in situ observations. The location of the stations is also limited as some of the closest usable precipitation stations are a significant distance away from streamflow stations (Appendix 1). The TRMM data has a very large grid spacing, which in the small study area tended to be about four pixels, which was very limiting for the analysis of the mesoscale convection that occurs daily in the region. Flow stations within the watershed are few and, due to possible errors in the DEM analysis, do not appear on streams as output by ArcGIS.

In addition, the stations used are clustered in lower elevation areas with only five on a slope greater than 20°. In these shallower slope areas, it is possible that the same storm

will have an effect on several areas. This may cause an addition problem for the comparison of streamflow and precipitation because low area streams may be strongly affected by precipitation high in the mountains. Additionally with the sparse data available over the steeper terrain it is difficult to evaluate at how much the mountain ranges influence the streamflow, especially as some of the precipitation stations are on the opposite side of the mountain to the streamflow stations.

### **Future Work**

The goal of the slope-precipitation-stream flow analysis is to improve flood prediction and warning capabilities. The flood risk indices created from this project are to be applied to an interactive map on IDEAM's publicly accessible website. Additionally, this map can have TRMM precipitation data and DRIVE flooding information overlaid, and provide flood warnings using these two pieces of information. The same information is intended to be used in the Mi Pronóstico mobile phone app. The mobile app would have the additional capability of directing the user to safety in the case of a flood. These safe areas could be determined using the calculated flood risk indices. The vulnerability is also dependent on the development and land use of the floodplain. Therefore, in the future, it would be beneficial to develop a more sophisticated risk analysis using the population and land usage in flood basins [Künzler, Huggel, and Ramírez, 2012].

### **V. Conclusions**

As there is a low index of variability for the stations within the La Mosca watershed and a moderate MCTI, the overall risk of La Mosca Watershed is moderate. Therefore, in events where there is heavy precipitation over the area La Mosca river basin will be at a medium risk for flooding. The process has been automated in order for it to be run for different watersheds and any number of sub basins. The pour points have to be placed by the user manually before the program can be run, and the TRMM and DRIVE model data must be pulled off line and input into ArcMap, but allow for a more dynamic view of flood risks.

The web application can be updated to include this information on a map and will allow for users to view their area for flood risk as well as what the current conditions are. Once this product is linked to the Mi Pronóstico web application it will be extremely helpful to individuals, businesses, city planners, and emergency management for Colombia. The methodology can be expanded to other watersheds throughout Colombia. It can then be updated into the format of the mobile Mi Pronóstico application to give users flood warnings and identify locations where safe areas and shelters are located.

### **VI. Acknowledgments**

The DEVELOP Tech Team would like to thank NASA DEVELOP as well as our science advisors Lauren Childs-Gleason and Dr. Kenton Ross for working with us this term at DEVELOP. We would also like to thank Dr. Angelica Gutierrez for being our point of contact and translator to the team in IDEAM as well as for her support throughout the

project. We would like to thank our partners in Colombia at IDEAM, Pilar Galindo and Ricardo Quiroga for their data and support throughout the term.

## VII. References

- Bookhagen, B. and D. W. Burbank (2006), Topography, relief, and TRMM-derived rainfall variations along the Himalaya, *Geophysical Research Letters*, 33, 1-5, doi:10.1029/2006GL026037
- Colombia-SA, (2014), Antioquia. Accessed on June 23, 2014 from: <http://www.colombia-sa.com/departamentos/antioquia/antioquia-in.html>
- Czubski, K., J. Kozak, and, N. Kolecka (2013), Accuracy of SRTM-X and ASTER Elevation Data and its Influence on Topographical and Hydrological Modeling: Case Study of the Pieniny Mts. in Poland, *International Journal of Geoinformatics*, 9, 7-14
- Dinku, T., F. Ruiz, S.J. Connor, and P. Ceccato (2009), Validation and intercomparison of satellite rainfall estimates over Colombia, *Journal of Applied Meteorology and Climatology*, 49, 1004 - 1014, doi:10.1175/2009JAMC2260.1.
- Friendly, M. (2002), Corgrams: Exploratory displays for correlation matrices, *The American Statistician*, 1.5, 1-16.
- Hijmans, R. (2014), DIVA-GIS, Colombia Administrative Areas and Inland Water. Accessed on June 23, 2014 from: <http://www.diva-gis.org/gdata>
- Hirano, A. Welch, R. Lang, H. (2002), Mapping from ASTER stereo image data: DEM validation and accuracy assessment, Center for Remote Sensing and Mapping Science (CRMS), Department of Geography, The University of Georgia
- Huffman, G.J., D.T. Bolvin, E.J. Nelkin, and R.F. Adler (2014), Experimental Real-time TRMM Multi-Satellite Precipitation Analysis (TMPA-RT): 3B42RT. Accessed from: [http://gdata1.sci.gsfc.nasa.gov/daac-bin/G3/gui.cgi?instance\\_id=TRMM\\_3B42RT](http://gdata1.sci.gsfc.nasa.gov/daac-bin/G3/gui.cgi?instance_id=TRMM_3B42RT)
- Kawanishi, T., H. Kuroiwa, M. Kojima, K. Oikawa, T. Kozu, H. Kumagai, K. Okamoto, M. Okumura, H. Hakatsuka, and K. Nishikawa (2000), TRMM Precipitation Radar, *Advance Space Research*, 25, 969-972.
- Künzler, M., C. Huggel, and J.M. Ramírez (2012), A risk analysis for floods and lahars: case study in the Cordillera Central of Colombia, *Natural Hazards*, 64, 767-796. doi: 10.1007/s11069-012-0271-9
- Land Processes Distributed Active Archive Center. Routine ASTER Global Digital Elevation Model. Accessed on June 23, 2014 from: [https://lpdaac.usgs.gov/products/aster\\_products\\_table/astgtm](https://lpdaac.usgs.gov/products/aster_products_table/astgtm)
- Mosquera-Machado, S. and S. Ahmad (2007), Flood hazard assessment of Atrato River in Colombia, *Water Resource Management*, 21, 591-609, doi: 10.1007/s11269-006-9032-4.
- Mrekva, L. and Z. Engi (2012), Urban flood risk and hydrology, Lower-Danube-Valley Directorate for Environment and Water, West-Transdanubian environmental and Water Directorate.

- Nikolakopoulos, K. G. E. K. Kamaratakis, N. Chrysoulakis (2006), SRTM vs ASTER elevation products. Comparison for two regions in Crete, Greece, *International Journal of Remote Sensing*, 27, 4819-4838
- Poveda, G., D.M. Álvarez, and Ó.A. Rueda (2011), Hydro-climatic variability over the Andes of Colombia associated with ENSO: a review of climatic processes and their impact on one of the Earth's most important biodiversity hotspots, *Climate Dynamics*, 36, 2233-2249.
- Poveda, G., O.J. Mesa, L.F. Salazar, P.A. Arias, H.A. Moreno, S.C. Viera, P.A. Agudelo, V.G. Toro, and J.Felipe Alvarez (2005), The diurnal cycle of precipitation in the tropical Andes of Colombia, *Monthly Weather Review*, 133, 228-240.
- Rasmussen, K.L., S.L. Choi, M.D. Zuluaga, and R.A. Houze, Jr. (2013), TRMM precipitation bias in extreme storms in South America, *Geophysical Research Letters*, 40, 3457-3461, doi: 10.1002/grl.50651.
- Rodríguez, E., C.S. Morris, J.E. Belz, E.C. Chapin, J.M. Martin, W. Daffer, S. Hensley, 2005, An assessment of the SRTM topographic products, Technical Report JPL D-31639, Jet Propulsion Laboratory, Pasadena, California, 143 pp.
- Spachinger, K., W. Dorner, R. Metzka, K. Serrhini, and S. Fuchs (2008), Flood risk and flood hazard maps - Visualization of hydrological risks, IOP Conference Series: Earth and Environmental Science, 4, doi: 10.1088/1755-1307/4/1/012043
- Tachikawa, T., M. Kaku, A. Iwasaki, D. Gesch, M. Oimoen, Z. Zhang, J. Danielson, T. Krieger, B. Curtis, J. Haase, M. Abrams, R. Crippen, C. Carabajal (2011), ASTER Global Digital Elevation Model Version 2 - Summary of Validation Results, NASA Land Processed Distributed Active Archive Center, Joint Japan-US ASTER Science Team
- Tighe, M. L. D. Chamberlain (2009), Accuracy Comparison of the SRTM, ASTER, NED, NEXTMAP, USA Digital Terrain Model Over Several USA Study Sites, ASPRS/MAPPS 2009 Fall Conference, San Antonio, Texas.
- Wu, H. (2014), Global Flood Monitoring System. Accessed on July 14, 2014 from: flood.umd.edu
- Wu, H., R.F. Adler, Y. Tian, G.J. Huffman, H. Li, and J. Wang (2014), Real-time global flood estimation using satellite-based precipitation and a coupled land surface and routing model, *Water Resources Research*, 50, 2693-2717, doi:10.1002/2013WR014710.
- Zhao, G. Xue, H. Ling, F. (2010), Assessment of ASTER GDEM Performance by Comparing with SRTM and ICESat/GLAS Data in Central China, Institute of Geodesy and Geophysics, Chinese Academy of Sciences
- Unpublished sources:  
 IDEAM, MAVDT, (2013) Lineamientos conceptuales y metodológicos para la Evaluación Regional del Agua ERA
- Tarpey, T. (2013) Time Series Analysis, accessed on June 25, 2014 from: <http://www.wright.edu/~thaddeus.tarpey/ES714timeseries.pdf>

## VIII. Appendices

### Appendix 1:

	Daily Correlation	Monthly Correlation
Streamflow Station Identifier	Streamflow and Precipitation	Streamflow and Precipitation
23087010	0.43	0.68
23087020	0.35	0.74
23087030	0.42	0.67
23087040	0.37	0.80
23087060	0.51	0.78
23087080	0.29	0.68
23087090	0.34	0.68
23087100	0.18	0.70
23087130	0.54	0.67
23087150	0.25	0.58
23087170	0.45	0.68
23087180	0.18	0.45
23087190	0.16	0.49
23087200	0.16	0.56
23087210	0.12	0.44
23087690	0.26	0.69
23087700	0.19	0.38
23087740	0.32	0.73
23087830	0.19	0.53

Correlations between streamflow and precipitation slope for 19 combination precipitation and streamflow stations.

Stream Flow Station	Precipitation Station	Distance Between (KM)	Stream Flow Station	Precipitation Station	Distance Between (KM)	Stream Flow Station	Precipitation Station	Distance Between (KM)
23087010	23080210	1.82433687	23087180	23080680	1.5091696	23087700	23080640	1.48176667
23087020	23080340	1.8491406	23087190	23080160	8.72947549	23087710	23080350	1.8491406
23087030	23080220	6.68010951	23087200	23085140	2.12371292	23087720	23080350	1.8491406
23087040	23080270	2.60631301	23087210	23080720	0.10968285	23087730	23080290	2.60639067
23087050	23080950	4.11991656	23087260	23080270	2.1788916	23087740	23085200	1.03625426
23087060	23085050	1.84902966	23087300	23080270	1.39257768	23087770	23080150	2.58163304
23087080	23080210	0	23087460	23085010	0	23087780	23080210	1.82433687
23087090	23080340	2.61908978	23087470	23080470	1.08051902	23087790	23080300	1.8491406
23087100	23085190	0	23087630	23080190	4.09513769	23087800	23080340	1.85424748
23087110	23080940	0.38285586	23087640	23080570	4.13749914	23087810	23080290	0
23087120	23080690	0	23087650	23080430	4.14310778	23087820	23080350	0
23087130	23080430	1.85435874	23087660	23080170	0.83303199	23087830	23080640	4.02337916
23087150	23080270	1.64044937	23087670	23080270	3.51743822	23087860	23080220	1.84902966
23087160	23080030	3.56893002	23087680	23080060	2.61937321			
23087170	23080220	0	23087690	23085200	1.03625426			

Distance between the closest precipitation and streamflow station in kilometers.

Appendix 2:

Below are the untranslated charts for Figure 1 and Tables 1-3.

Índice morfométrico	Escala	Área de la cuenca de drenaje (km <sup>2</sup> )	Categorías				
			1	2	3	4	5
Densidad de drenaje (km/km <sup>2</sup> )	1:10.000	<15	<1,50	1,51 – 2,00	2,01 – 2,50	2,51 – 3,00	> 3
	1:25.000	16 a 50	<1,20	1,21 – 1,80	1,81 – 2,00	2,01 – 2,50	> 2,5
	1:100.000	>50	<1,00	1,01 – 1,50	1,51 – 2,00	2,01 – 2,50	> 2,5
			Baja	Moderada	Moderada Alta	Alta	Muy Alta
Pendiente media de la cuenca (%)	1:10.000	<15	<20	21 – 35	36 – 50	51 – 75	>75
	1:100.000	>50	<15	16 – 30	30 – 45	46 – 65	>65
			Accidentado	Fuerte	Muy Fuerte	Escarpado	Muy Escarpado
Coeficiente de compacidad			<1,625	1,376 -1,500	1,251- 1,375	1,126 – 1,250	1,00 – 1,125
			Oval-oblonga a rectangular-oblonga	Oval-redonda a oval-oblonga	Casi redonda a oval-redonda		

Untranslated Table 1. Morphometric Indices.

		Pendiente media de la cuenca						
		1	2	3	4	5		
Densidad de drenaje	1	111	121	131	141	151	1	Coeficiente de forma
		112	122	132	142	152	2	
		113	123	133	143	153	3	
		114	124	134	144	154	4	
		115	125	135	145	155	5	
	2	211	221	231	241	251	1	
		212	222	232	242	252	2	
		213	223	233	243	253	3	
		214	224	234	244	254	4	
		215	225	235	245	255	5	
	3	311	321	331	341	351	1	
		312	322	332	342	352	2	
		313	323	333	343	353	3	
		314	324	334	344	354	4	
		315	325	335	345	355	5	
	4	411	421	431	441	451	1	
		412	422	432	442	452	2	
		413	423	433	443	453	3	
		414	424	434	444	454	4	
		415	425	435	445	455	5	
	5	511	521	531	541	551	1	
		512	522	532	542	552	2	
		513	523	533	543	553	3	
		514	524	534	544	554	4	
		515	525	535	545	555	5	

Untranslated Figure 1: Morphometric index of torrential events.

Muy alta    
  Baja    
  Muy baja  
 Alta    
  Moderada

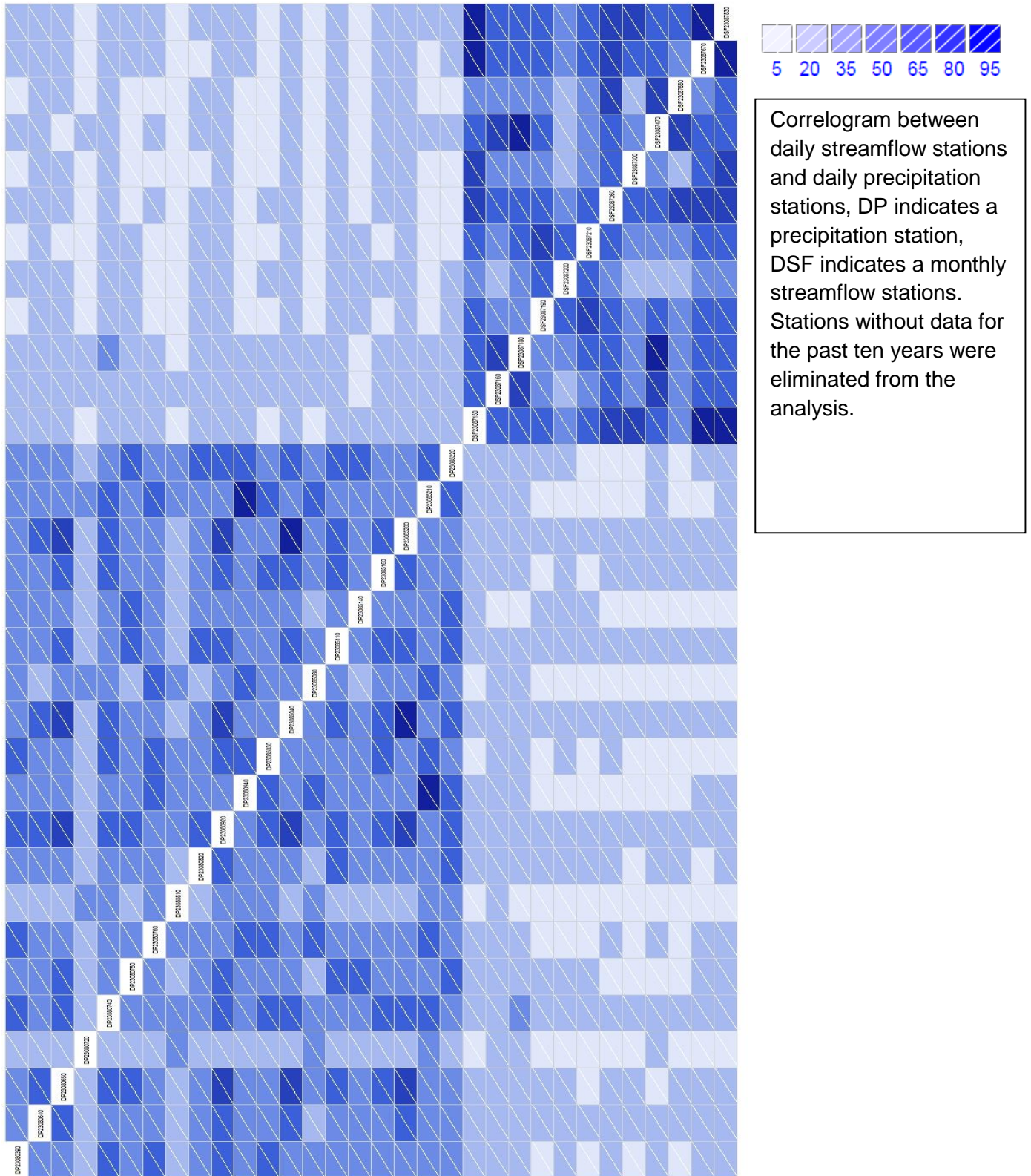
Índice de variabilidad	Vulnerabilidad
< 10°	Muy baja
10.1° - 37°	Baja
37.1° - 47°	Media
47.1° - 55	Alta
>55°	Muy alta

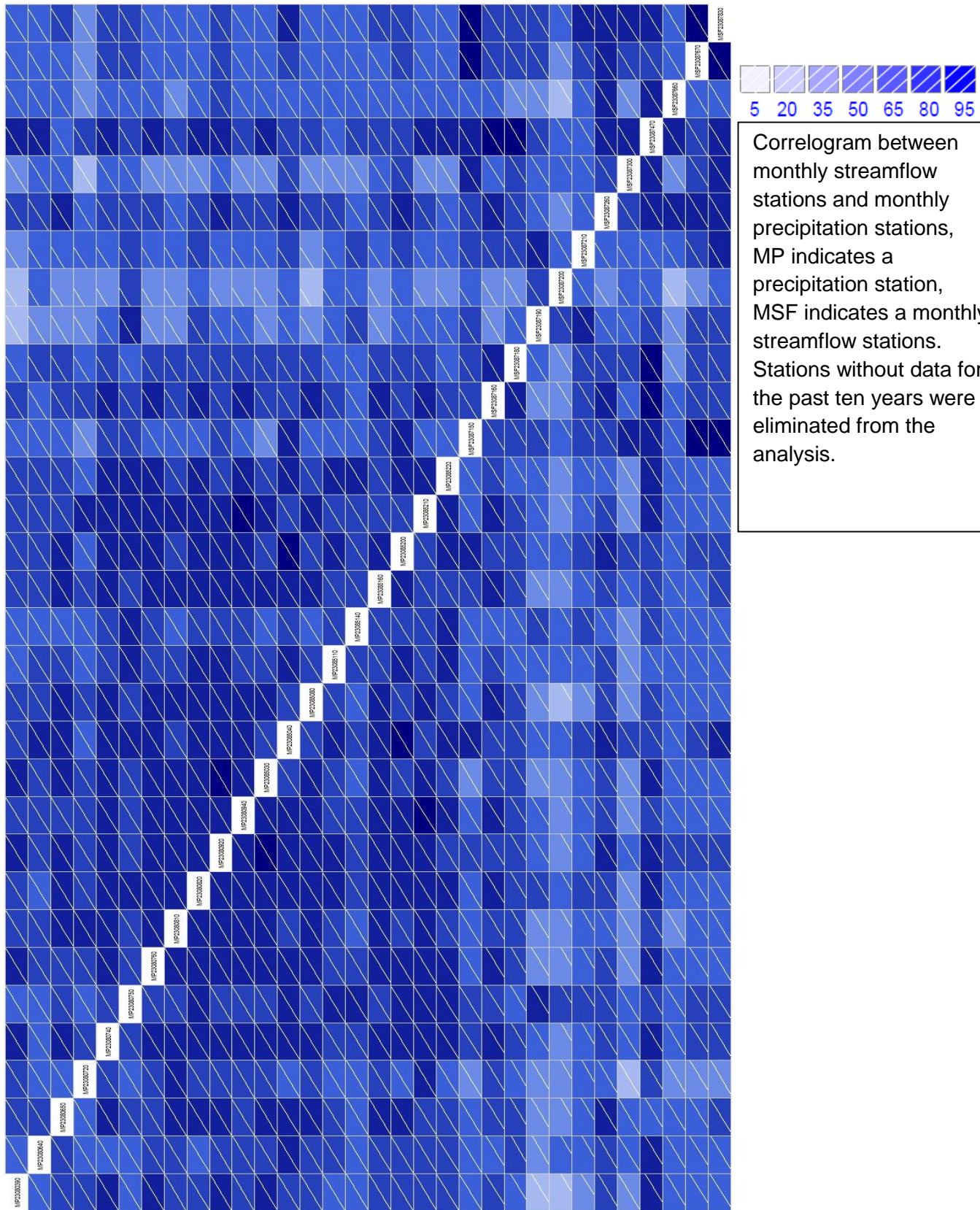
Untranslated Table 2: Index of variability classification.

Índice de variabilidad	Índice morfométrico de torrencialidad				
	Muy baja	Baja	Media	Alta	Muy alta
Muy baja	Baja	Baja	Media	Alta	Alta
Baja	Baja	Media	Media	Alta	Muy alta
Media	Baja	Media	Alta	Alta	Muy alta
Alta	Media	Media	Alta	Muy alta	Muy alta
Muy alta	Media	Alta	Alta	Muy alta	Muy alta

Untranslated Table 3: Vulnerability classification that will be seen by users in Colombia.

Appendix 3:





Correlogram between monthly streamflow stations and monthly precipitation stations, MP indicates a precipitation station, MSF indicates a monthly streamflow stations. Stations without data for the past ten years were eliminated from the analysis.

**REPORT DOCUMENTATION PAGE**

*Form Approved  
OMB No. 0704-0188*

The public reporting burden for this collection of information is estimated to average 1 hour per response, including the time for reviewing instructions, searching existing data sources, gathering and maintaining the data needed, and completing and reviewing the collection of information. Send comments regarding this burden estimate or any other aspect of this collection of information, including suggestions for reducing this burden, to Department of Defense, Washington Headquarters Services, Directorate for Information Operations and Reports (0704-0188), 1215 Jefferson Davis Highway, Suite 1204, Arlington, VA 22202-4302. Respondents should be aware that notwithstanding any other provision of law, no person shall be subject to any penalty for failing to comply with a collection of information if it does not display a currently valid OMB control number.  
**PLEASE DO NOT RETURN YOUR FORM TO THE ABOVE ADDRESS.**

<b>1. REPORT DATE (DD-MM-YYYY)</b> 01-09-2014		<b>2. REPORT TYPE</b> Contractor Report		<b>3. DATES COVERED (From - To)</b>	
<b>4. TITLE AND SUBTITLE</b>  Colombia Mi Pronóstico Flood Application: Updating and Improving the Mi Pronóstico Flood Web Application to Include an Assessment of Flood Risk				<b>5a. CONTRACT NUMBER</b> NNX14AB604	
				<b>5b. GRANT NUMBER</b>	
				<b>5c. PROGRAM ELEMENT NUMBER</b>	
				<b>5d. PROJECT NUMBER</b>	
<b>6. AUTHOR(S)</b>  Rushley, Stephanie; Carter, Matthew; Chiou, Charles; Farmer, Richard; Haywood, Kevin; Pototzky, Anthony, Jr.; White, Adam; Winker, Daniel				<b>5e. TASK NUMBER</b>	
				<b>5f. WORK UNIT NUMBER</b> 389018.02.14.01.05	
				<b>8. PERFORMING ORGANIZATION REPORT NUMBER</b>	
<b>7. PERFORMING ORGANIZATION NAME(S) AND ADDRESS(ES)</b> NASA Langley Research Center Hampton, Virginia 23681				<b>10. SPONSOR/MONITOR'S ACRONYM(S)</b>  NASA	
<b>9. SPONSORING/MONITORING AGENCY NAME(S) AND ADDRESS(ES)</b> National Aeronautics and Space Administration Washington, DC 20546-0001				<b>11. SPONSOR/MONITOR'S REPORT NUMBER(S)</b> NASA/CR-2014-218526	
<b>12. DISTRIBUTION/AVAILABILITY STATEMENT</b> Unclassified - Unlimited Subject Category 43 Availability: NASA CASI (443) 757-5802					
<b>13. SUPPLEMENTARY NOTES</b>  Langley Technical Monitor: Lindsay M. Rogers					
<b>14. ABSTRACT</b>  Colombia is a country with highly variable terrain, from the Andes Mountains to plains and coastal areas, many of these areas are prone to flooding disasters. To identify these risk areas NASA's Advanced Spaceborne Thermal Emission and Reflection Radiometer (ASTER) was used to construct a digital elevation model (DEM) for the study region. The preliminary risk assessment was applied to a pilot study area, the La Mosca River basin. Precipitation data from the National Aeronautics and Space Administration (NASA) Tropical Rainfall Measuring Mission (TRMM)'s near-real-time rainfall products as well as precipitation data from the Instituto de Hidrologia, Meteorologia y Estudios Ambientales (the Institute of Hydrology, Meteorology and Environmental Studies, IDEAM) and stations in the La Mosca River Basin were used to create rainfall distribution maps for the region. Using the precipitation data and the ASTER DEM, the web application, Mi Pronóstico, run by IDEAM, was updated to include an interactive map which currently allows users to search for a location and view the vulnerability and current weather and flooding conditions. The geospatial information was linked to an early warning system in Mi Pronóstico that can alert the public of flood warnings and identify locations of nearby shelters.					
<b>15. SUBJECT TERMS</b>  Correlation; Flooding risk; Precipitation; Risk assessment; Streamflow; TRMM					
<b>16. SECURITY CLASSIFICATION OF:</b>			<b>17. LIMITATION OF ABSTRACT</b>	<b>18. NUMBER OF PAGES</b>	<b>19a. NAME OF RESPONSIBLE PERSON</b>
<b>a. REPORT</b>	<b>b. ABSTRACT</b>	<b>c. THIS PAGE</b>			STI Help Desk (email: help@sti.nasa.gov)
U	U	U	UU	27	<b>19b. TELEPHONE NUMBER (Include area code)</b> (443) 757-5802